S Supplementary Information

S.1 Flowchart of the analytic algorithm

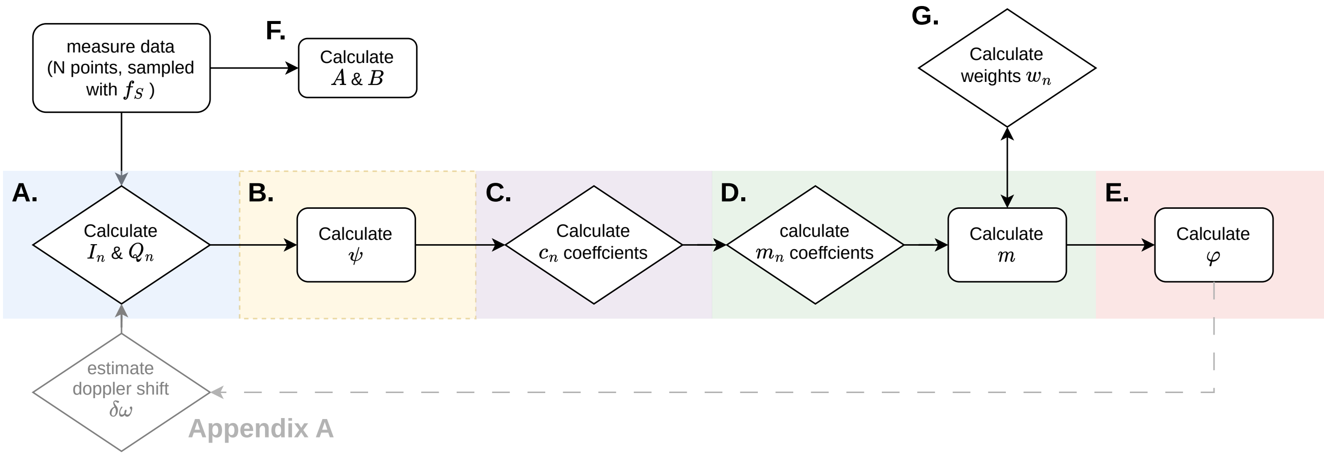

Figure S.1. Flowchart of the analytic algorithms. The grey dashed lines correspond to additional calculation steps explained in 5.1 for the case of a dynamic signal.

S.2 Algorithm relations to Deep-Phase Modulation (DPM) Interferometry

The predecessor of DFMI, Deep-Phase modulation interferometry (**DPMI**) introduced by Heinzel et al. has an almost identical signal to DFMI. In a DPMI setup as shown in Figure S.2, the phase modulation index m does not scale with the interferometers arm-length difference ΔL. Here a sinusodial modulation is introduced to the signal with the intend to create higher order harmonics, which also carry the microscopic distance / the phase information of the arm-length difference. When the arm-length difference changes, the modulation index remains constant. The analytic readout algorithm we present here works however the same on both DFMI and DPMI signals. Only the physical interpretation on the calculated coefficients differs.

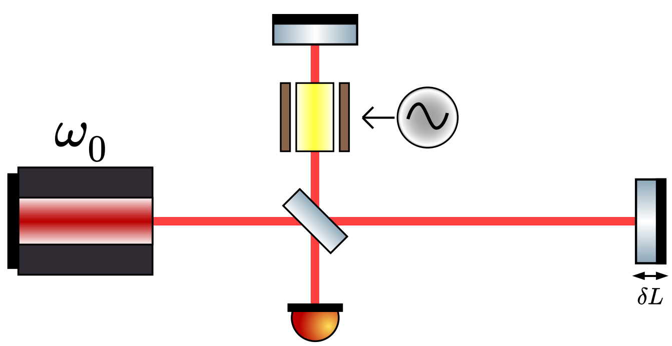

Figure S.2. Sketch of a DPMI setup. Here, only the relative changes of the arm-length differene / the test-mass position can be measured with high precision.

S.3 On the effect of different window-function for a DFM signal

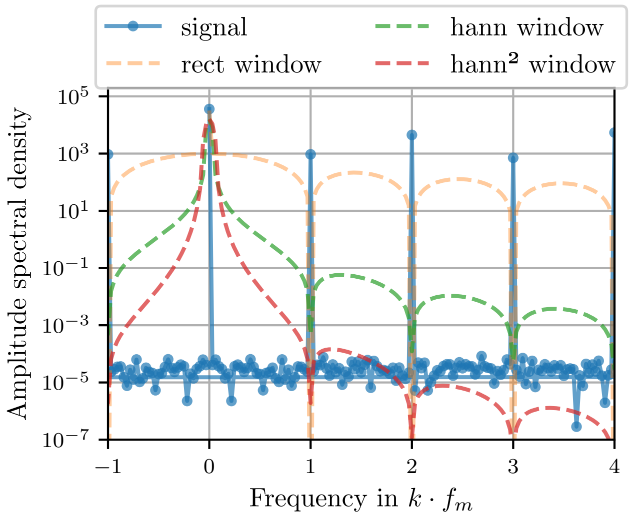

Figure S.3. Fourier transform of the signal and different window functions for one modulation period ($T = 2\pi/\omega_m$). In the I-Q-Demodulation scheme, the demodulated expression must be low-pass filtered (in this case by applying a window function and integrating the time-series) to suppress the contribution of the $k \neq 0$ harmonics. The window functions shown here all have zeros at multiples of the modulation frequency ω_m.

S.4 Dynamic Readout Extension

Figure S.4 shows a sketch of the demodulation scheme for the splitted tones / harmonics of a dynamic signal as introduced in section 5. Here the frequency shift $\delta\omega$ must be known in the beginning of the algorithm to demodulate the harmonics correctly at their shifted frequencies.

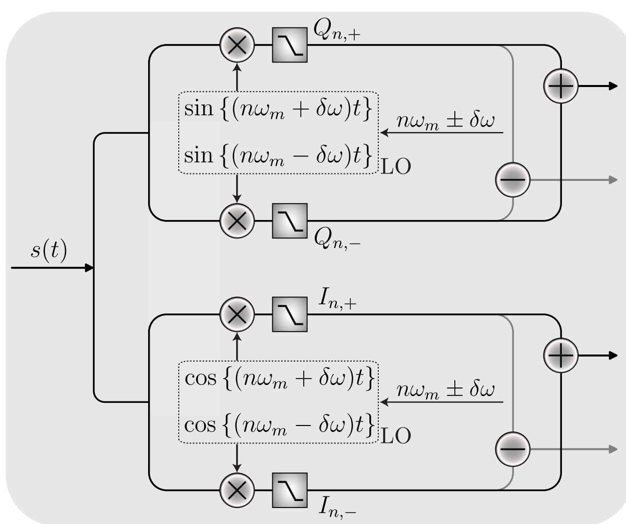

Figure S.4. Sketch of the demodulation scheme of the n'th harmonic. In the algorithm, this part is present multiple times up to the number of harmonics visible above the noise floor.

S.4.1 Additional coefficients used in the dynamic readout

The modified I_n and Q_n coefficients for the dynamic readout can be seen in table S.1. From these, additional intermediate coefficients are calculated an seen in table S.2 which are used to calculate the signal parameters as outlined in section 5.1.

low-pass filter of	=:	
$s(t)\cdot\sin((n\omega_m+\delta\omega)t)$	$Q_{n,+}$	$\frac{A}{2}\cdot J_n(m)\cdot\big[-\big(\sin\varphi-(-1)^k\sin(\delta\omega T+\varphi)\mathrm{sinc}(\delta\omega T)\big)\cos(k\psi) - \big(\cos\varphi+(-1)^k\cos(\delta\omega T+\varphi)\mathrm{sinc}(\delta\omega T)\big)\sin(k\psi)\big]$
$s(t)\cdot\sin((n\omega_m-\delta\omega)t)$	$Q_{n,-}$	$(-1)^k\cdot\frac{A}{2}\cdot J_n(m)\cdot\big[+\big(\sin\varphi-(-1)^k\sin(\delta\omega T+\varphi)\mathrm{sinc}(\delta\omega T)\big)\cos(k\psi) - \big(\cos\varphi+(-1)^k\cos(\delta\omega T+\varphi)\mathrm{sinc}(\delta\omega T)\big)\sin(k\psi)\big]$
$s(t)\cdot\cos((n\omega_m+\delta\omega)t)$	$I_{n,+}$	$\frac{A}{2}\cdot J_n(m)\cdot\big[-\big(\sin\varphi-(-1)^k\sin(\delta\omega T+\varphi)\mathrm{sinc}(\delta\omega T)\big)\sin(k\psi) + \big(\cos\varphi+(-1)^k\cos(\delta\omega T+\varphi)\mathrm{sinc}(\delta\omega T)\big)\cos(k\psi)\big]$
$s(t)\cdot\cos((n\omega_m-\delta\omega)t)$	$I_{n,-}$	$(-1)^k\cdot\frac{A}{2}\cdot J_n(m)\cdot\big[+\big(\sin\varphi-(-1)^k\sin(\delta\omega T+\varphi)\mathrm{sinc}(\delta\omega T)\big)\sin(k\psi) + \big(\cos\varphi+(-1)^k\cos(\delta\omega T+\varphi)\mathrm{sinc}(\delta\omega T)\big)\cos(k\psi)\big]$

Table S.1. Table of the I_n and Q_n coefficients obtained from the I-Q-demodulation of the different DFM harmonics for non-negligible frequency shifts $\delta\omega$.

	n even	n odd
$(Q_{n,+}+Q_{n,-})$	$-AJ_k(m)\Big(\cos\varphi+\cos(\delta\omega T+\varphi)\mathrm{sinc}(\delta\omega T)\Big)\sin(k\psi)$	$-AJ_k(m)\Big(\sin\varphi+\sin(\delta\omega T+\varphi)\mathrm{sinc}(\delta\omega T)\Big)\cos(k\psi)$
$(I_{n,+}+I_{n,-})$	$AJ_k(m)\Big(\cos\varphi+\cos(\delta\omega T+\varphi)\mathrm{sinc}(\delta\omega T)\Big)\cos(k\psi)$	$-AJ_k(m)\Big(\sin\varphi+\sin(\delta\omega T+\varphi)\mathrm{sinc}(\delta\omega T)\Big)\sin(k\psi)$
$(Q_{n,+}-Q_{n,-})$	$-AJ_k(m)\Big(\sin\varphi-\sin(\delta\omega T+\varphi)\mathrm{sinc}(\delta\omega T)\Big)\cos(k\psi)$	$-AJ_k(m)\Big(\cos\varphi-\cos(\delta\omega T+\varphi)\mathrm{sinc}(\delta\omega T)\Big)\sin(k\psi)$
$(I_{n,+}-I_{n,-})$	$-AJ_k(m)\Big(\sin\varphi-\sin(\delta\omega T+\varphi)\mathrm{sinc}(\delta\omega T)\Big)\sin(k\psi)$	$AJ_k(m)\Big(\cos\varphi-\cos(\delta\omega T+\varphi)\mathrm{sinc}(\delta\omega T)\Big)\cos(k\psi)$
$c_{n,+}$	$AJ_k(m)\Big(\cos\varphi+\cos(\delta\omega T+\varphi)\mathrm{sinc}(\delta\omega T)\Big)$	$AJ_k(m)\Big(\sin\varphi+\sin(\delta\omega T+\varphi)\mathrm{sinc}(\delta\omega T)\Big)$
$c_{n,-}$	$AJ_k(m)\Big(\sin\varphi-\sin(\delta\omega T+\varphi)\mathrm{sinc}(\delta\omega T)\Big)$	$AJ_k(m)\Big(\cos\varphi-\cos(\delta\omega T+\varphi)\mathrm{sinc}(\delta\omega T)\Big)$

Table S.2. Table of additional coefficients derived from table S.1.